

NC 9-40202
NASA CR-66803

EXPERIMENTS ON MAGNETOPLASMA DYNAMIC
ENGINES WITH ROTATING CURRENT
DISTRIBUTIONS
By A. V. Larson

ution of this report is provided in the

CASE FILE
COPY

GENERAL DYNAMICS
Convair Division

EXPERIMENTS ON MAGNETOPLASMA DYNAMIC
ENGINES WITH ROTATING CURRENT
DISTRIBUTIONS

By A. V. Larson

Distribution of this report is provided in the interest of information exchange. Responsibility for the contents resides in the author or organization that prepared it.

Prepared under Contract NAS 1-8028 by
Convair Division of General Dynamics
San Diego, California

for

NATIONAL AERONAUTICS AND SPACE ADMINISTRATION
Langley Research Center
Langley Station
Hampton, Virginia 23365

June 1969

ABSTRACT

Flow properties within a continuous d.c. magnetoplasma dynamic engine have been investigated by measuring the ion saturation current to a planar Langmuir probe as a function of probe orientation and position. Plasma swirl, its helical pitch, and its degree of azimuthal uniformity are easily identified. Striking differences occur if the thruster has an axisymmetric electric current distribution or a rotating current spoke. The Langmuir probe appears to detect rotating spokes almost as well as do Rogowski coils wrapped around the thruster anode segments. Transition thresholds from the spoke to no-spoke modes, both visibly stable, are observed, as moderate changes of 10 to 20% are made in either arc current, mass flow or magnetic field. Thermal efficiencies are slightly better on the spoke side of the transition threshold. The arc voltage and the average azimuthal plasma flow change little at the onset of the spoke.

The arc parameters were 100 to 600 amp, 10 to 40 mg/sec of argon, and bias magnetic fields up to 2700 gauss.

TABLE OF CONTENTS

	<u>Page</u>
I. INTRODUCTION	1
II. APPARATUS	2
III. EXPERIMENTS	6
1. Cathode at $z = 3.23$ cm	6
2. Cathode at other Positions	16
3. Effects of Anode Segments and Geometry	16
IV. CONCLUSIONS	18
V. ACKNOWLEDGEMENTS	19
VI. REFERENCES	20
APPENDIX I	21
1. Pneumatic Actuator	21
2. Lever	22
3. Stop Wheel	22
4. Probe Angle Control	22
5. Probe Angle Indicator	22
6. Apparatus Mount	22
7. Material	22

LIST OF ILLUSTRATIONS

<u>Figure</u>		<u>Page</u>
1.	Thruster and probe.	3
2.	Anode segments and Langmuir probe.	4
3.	Cathode and probe midsection.	5
4.	Evidence for onset of rotating spoke.	7
5.	Thruster modes and anode power loss.	9
6.	Anode loss and voltage vs. B_z .	10
7.	Segment current vs. time at various mass flow rates.	12
8.	J_2 and J_3 vs. α .	13
9.	Ion flow in the θ - z plane vs. position: axial component and off axis angle.	14
10.	Ion flow in the θ - z plane vs. position: magnitude of the directed and random flows.	15
11.	Spoke onset, argon: cathode at $z = 2.54$ cm.	17
12.	Probe insertion apparatus.	23
13.	Experimental set up.	24

I. INTRODUCTION

Magnetoplasmadynamic (MPD) arc engines⁽¹⁾ usually have coaxial, axisymmetric electrodes between which propellant is accelerated. Conceptually, the electric current distribution between the electrodes can vary in azimuthal uniformity between the two extremes of either an axisymmetric distribution or a localized filament called a spoke. Since the thruster performance may be expected to depend upon the electric current distribution, it is important to determine any such correlations.

Recent work has demonstrated the existence of the spoke mode in both continuously running^(2,3,4) and pulsed, quasi-steady arcs.⁽⁵⁾ In all cases, an external magnetic field was applied and the spoke was observed to rotate. Malliaris⁽⁶⁾ has since determined that, if either the bias magnetic field is weaker than, say 500 gauss, or the arc current is stronger than 1000 amp, then a variety of indirect evidence for the existence of the spoke disappears. Theoretical treatment of such phenomena has been started.⁽⁷⁾

The spoke has been measured directly⁽⁸⁾ in a pulsed MPD device by use of small Rogowski loops in the discharge. In the same experiments, a double planar Langmuir probe, negatively biased, was used to determine the ion flux within the device. It was found that the rotating current spoke is also a rotating spoke of plasma, i.e., spatial azimuthal nonuniformity also exists in the plasma flow.

Our experiments are intended to investigate the properties of an engine running continuously with or without the presence of a spoke. The parameter region used is that one identified by Malliaris⁽⁶⁾ of weak applied magnetic field and moderate arc currents. We have found that the thruster runs very stably in either a spoke mode or a no-spoke mode.

Since the engine anode is segmented, the measurement of the current to each segment is a direct, sensitive indicator of the presence of the rotating spoke.⁽²⁾ The plasma flow is observed by a small double planar Langmuir probe which is rapidly inserted within the thruster and then withdrawn to avoid physical damage. The electrode losses are monitored calorimetrically by measuring the temperature rise of flowing coolant.

The operating conditions of the engine have been: propellant, argon; mass flow rate, 10 to 40 mg/sec; arc current, 100 to 600 amp; voltage, 25 to 34 v; bias magnetic field, 300 to 2700 gauss at the cathode tip.

II. APPARATUS

The engine which is presented by schematic in Figure 1 and by photograph in Figure 2 has been described previously in detail.⁽²⁾ The nozzle exit radius is 2.5 cm, the throat radius is 0.97 cm, and the cathode is 3.23 cm from the exit plane. Now the magnet has been moved upstream to allow the radial insertion of the Langmuir probe at various axial positions. The field angle is 20° from the z axis at the outer radius of the exit plane. The axial gaps in the three segment anode have narrow boron nitride spacers one of which is altered to accommodate changes in the axial position of the probe. Each anode segment is water cooled separately and has a separate electrical feed from a common bus. The time dependent component of the current to each segment is detected by Rogowski loops.⁽⁹⁾

Reference 2 also describes: the construction, calibration and use of the Rogowski loops; the magnet; the experimental facility; and the standard measurements. For the present experiments, Argon was the propellant and the operating tank pressure was near and below one **mtorr**.

Two schematic views of the double planar Langmuir probe are given in Figures 1 and 3. The shaft is a two-hole alumina tube, 1.5 mm in diameter, with the holes fused shut at the shaft tip. A platinum wire, 0.5 mm in diameter, is inserted in each hole. Away from the tip, on opposite sides of the shaft, two cuts are made perpendicular to the shaft axis. The shaft wall and one-half of each wire is cut away, to expose two parallel plane electrode surfaces flanked at each end by a semi-circle of metal. The semi-circles of wire at each end of the cuts are covered by glass fused to the alumina. The result is two parallel plane rectangular electrodes 0.5 mm by 1.5 mm in size.

Referring to Figure 1, the probe is placed within the thruster so that the midpoint of the midsection is at a known radial, r, and axial, z, distance from the center point of the exit plane. Referring to Figure 3, the ion saturation current densities J_2 and J_3 are separately measured. The electrodes are biased negatively, with respect to the cathode.

As the angle of rotation, α , of the probe about its own axis is changed, J_2 and J_3 will change, if the plasma is flowing. The ion flow angle, say α_1 , is easy to detect, for if $\alpha = \alpha_1$, then $J_2 = J_3$ because of symmetry. Then the direction and magnitude of the flow in the θ -z plane, $\vec{J}_{i\theta z}$, is determined from the difference, $J_2 - J_3$, at the angles $\alpha = \alpha_1 \pm 90^\circ$.

The electrodes are made parallel to within 2° . The calibration of the angle that the plane of the electrode surface makes with respect to the thruster axis is also good to 2° .

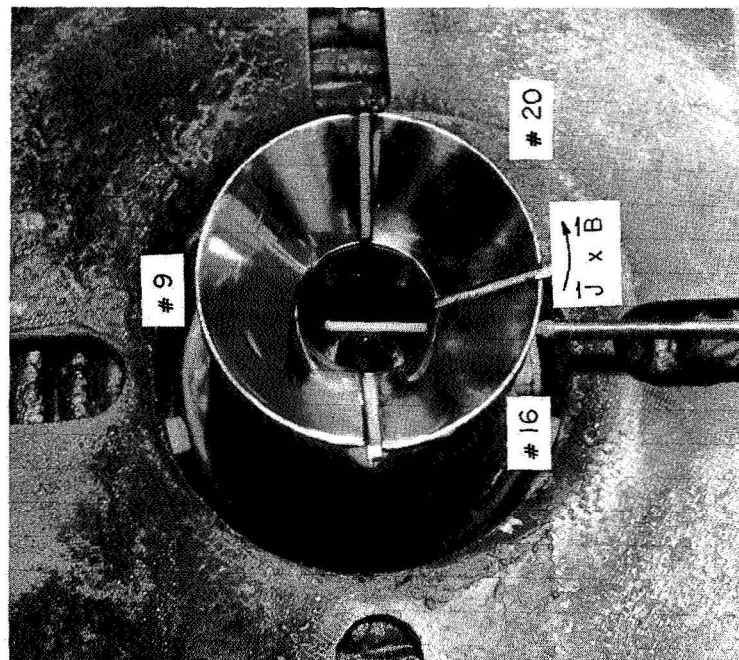


Figure 2. Anode segments and Langmuir probe.

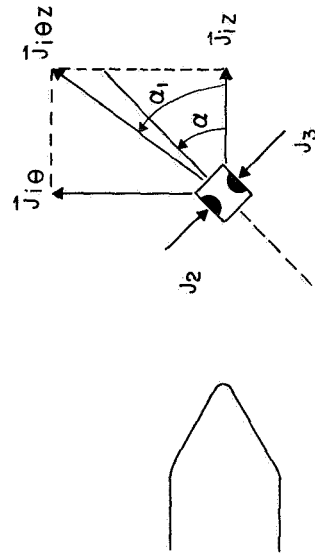


Figure 3. Cathode and probe midsection.
(top view)

The Langmuir probe theory is reviewed by Chen.⁽¹⁰⁾ It has been discussed in connection with MPD arcs by Brooks⁽¹¹⁾ and used by Burlock⁽¹²⁾ and Lovberg.⁽⁸⁾ The application within a continuously running engine is somewhat different. In order to prevent thermal damage, the probe is quickly inserted and withdrawn through a small hole in the boron nitride spacer. The exposure to the plasma varies from 5 to 50 msec. The mechanism for doing that is described in the appendix. Suffice it to say that α , r , z are well known, with the settings of the first two controlled from outside the vacuum tank. The axial position, z , is changed less frequently, and requires breaking vacuum.

III. EXPERIMENTS

1. Cathode at $z = 3.23$ cm

Most of the experiments were done with the cathode at $z = 3.23$ cm. Near the end of the contract the position was changed in order to effect better repeatability of some features of the measurements.

The first data concerns the identification of the thruster mode. Figure 4 gives typical evidence for two distinctly different modes. The top row shows the appearance of a rotating current spoke as B_z is changed from 960g to 1400g at the cathode tip. At the latter strength, a strong current channel passes from anode segment 9 to segment 16 periodically at a frequency of 77 kHz. At $B_z = 960$ g, there is no such phenomena, at any frequency. For the purpose of this report, the top photographs define the no-spoke and the spoke modes.

The second row in Figure 4 illustrates the Langmuir probe data. The electrodes are placed at $z = 1.6$ cm, their position in Figure 1, $r = 4$ mm, and $\alpha = 0^\circ$, the angular setting most sensitive to plasma swirling motion. In both modes, $J_3 - J_2$ is positive, indicating plasma swirl in the direction of the cross product of the arc current and applied magnetic field. In the spoke mode, the ion flux J_3 , to the probe facing upstream to the plasma swirl, is strongly modulated at the spoke frequency. The probe data and segment current data are taken simultaneously: The oscilloscope sweeps have identical time bases. The peak in the ion flux J_3 occurs as the electric current spoke sweeps past the probe, indicating a spatial correlation between the spoke and the plasma.

The third row gives J_3 and J_2 on a slower sweep, starting when the probe passes through the anode into the plasma. The probe radial position, $r(t)$, varies and the probe is in the plasma for 8 msec. The photographs show that the evidence for either mode is consistent at all radii.

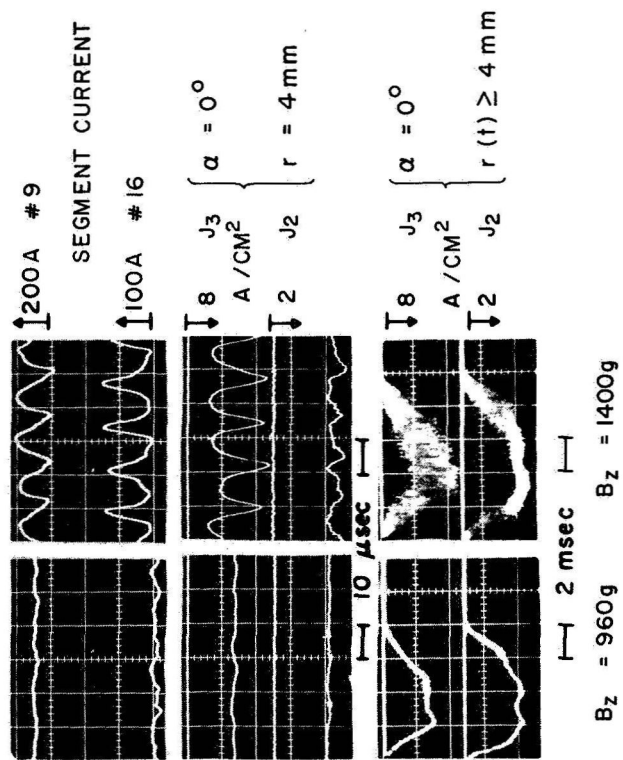


Figure 4. Evidence for onset of rotating spoke.
($I = 312 \text{ a}$, $M = 25 \text{ mg/sec}$, argon)

All the data in Figure 4 change appropriately if the magnetic field is reversed. The plasma swirl reverses direction, and, in the spoke mode, the spoke rotation reverses, and the strong ion flux modulation is then observed on J_2 . With either field direction, if the probe is placed on axis, $r = 0$, $\alpha = 0^\circ$, then $J_2 = J_3$. That is, there is no swirl on axis, as it should be, and in the spoke mode, modulations in J_2 or J_3 , if any, are minor. At any r , at $\alpha = \pm 90^\circ$, if the thruster is in the spoke mode, then strong modulations at the spoke frequency are observed also in the axial component of the ion flux, again mostly on the probe facing upstream. The evidence in this paragraph argues strongly against any spurious effects such as electrostatic pick up.

The double planar, negatively biased probe within the discharge thus appears to be a sensitive spoke detector. The probe and the segment current measurements then were used to identify the thruster mode as operating parameters were varied.

Figure 5 summarizes the data on thruster mode regions. Also some data points are given to show the percentage of arc power lost to the anode. The losses to the cathode were minor. The thruster mode regions are labelled according to this scheme:

S = well defined spoke, no fluctuations

N = no evidence of spoke, no fluctuations

T = transition between N and S

F = fluctuations

It is important to note that the engine was extremely stable in the N or S modes. No fluctuations were observed in the d.c. values of arc current, voltage, or jet luminosity. The two regions where fluctuations were sometimes observed are marked additionally with an F.

The transition region was found to wander along the B_z axis somewhat within a three-hour run, and more unpredictably from day to day. Always, however, the general pattern is the same as the one in Figure 5. For $\dot{m} = 15$ mg/sec, the transition region is most frequently nearer 600 to 700 gauss, and for $\dot{m} = 30$ mg/sec, it is nearer to 1500 to 1600 gauss, at the cathode tip. For a mass flow rate of 25 mg/sec, over many runs, the transition region has wandered over almost that same range. Two examples, at the extreme ends of the range, are given in Figure 6. Except for the voltage, the gross arc parameters were the same.

Figure 6 also illustrates that the transition from N to S can occur in two distinct ways. For the lower data, the transition from N to S is smooth, without visible fluctuation in luminosity or d.c. current or d.c. voltage. The data in the T region cannot be clearly described as representing either the N or the S mode. The trends of power loss and arc voltage with B_z are smooth.

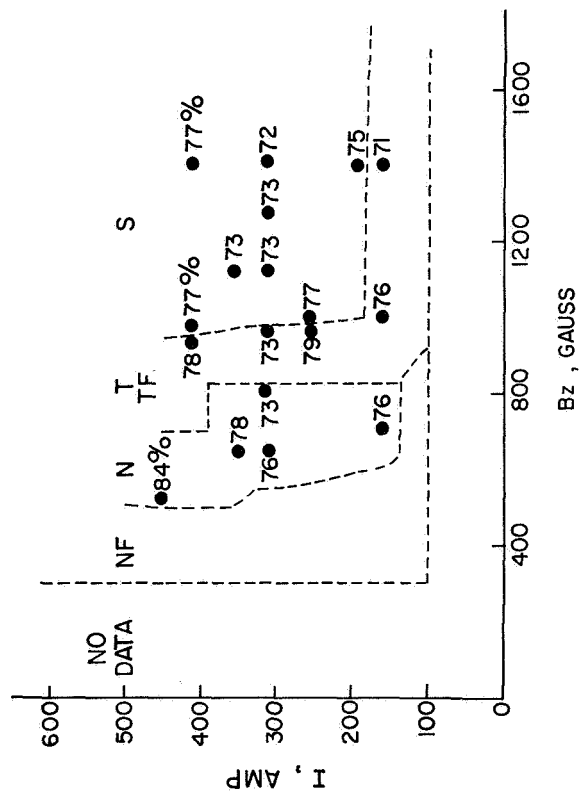


Figure 5. Thruster modes and anode power loss.
(M = 25 mg/sec, argon)

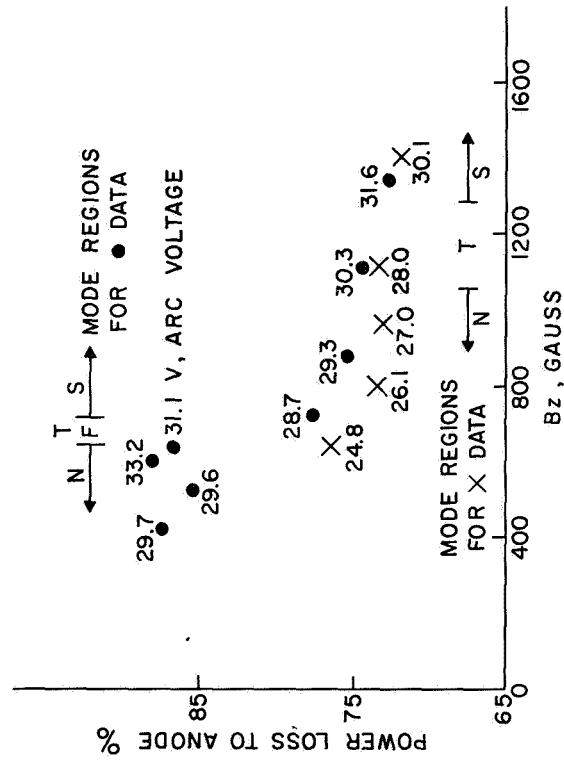


Figure 6. Anode loss and voltage vs. B_z .
($I = 312$ amp, $M = 25$ mg/sec argon)

For the upper data, the transition region is one in which the thruster is fluctuating between the N and the S mode. Alternately, it is definitely in one mode and then definitely in the other. The luminosity and the d.c. voltage and current all fluctuate. The trends of power loss and arc voltage change abruptly across the transition region. Here, there appears to be a close association between current distribution changes and the fluctuations and voltage mode changes that have been observed in all laboratories.

The patterns observed in Figures 5 and 6 have also been found in a like thruster with a solid anode. For that case, the probe is located just outside the exit plane. It is interesting to note that the N to S mode change is triggered by a 10 to 20% change in B_z . An example of data showing a mode change as the mass flow rate is varied by 10% from 31 to 28 mg/sec is given in Figure 7.

At the start of the program, the main goal was to relate eventually the plasma properties within the discharge to thrust production and to energy losses to the electrodes, for either a spoke or no-spoke mode. To this end, the double Langmuir probe was used to measure the θ , z components of the ion flux at fifteen points in a particular r - z plane within the thruster. The thruster was in a no-spoke mode, and the operating parameters were constant. At each point, the probe orientation angle, α , was varied from $+90^\circ$ to -90° . The data from three points is given in Figure 8 where J_2 and J_3 are plotted vs α . The angle at which $J_2 = J_3$ and through which $J_2 - J_3$ changes sign is easily identified. That is the swirl angle, α_1 , of Figure 3, which the ion flux makes with the thruster axis. Because of the probe symmetry, $J_2(\xi)$ should equal $J_3(-\xi)$, $\xi = \alpha - \alpha_1$, and the lines through the data are so drawn. At $\alpha = -90^\circ$ and $\alpha = 0^\circ$, the difference $J_3 - J_2$ gives the z and θ components, respectively, of the ion flux.

The method of presenting the map of the plasma flow in Figure 9 emphasizes the important thruster features, the ion flow along the line of thrust, J_{iz} , and the swirl angle, α_1 . Figures 9 and 10 should be read together, for the latter gives the magnitude of the flow along the ray α_1 , and also the random flux perpendicular to the ray. One observes relatively little plasma flow at the start of the cathode cone. In front of the cathode, the flow increases and the pattern is complicated. From there downstream, the axial ion flux integrated over a cross section of the jet continues to increase and the random currents continue to decrease. At the downstream throat edge, the flow is more uniform. Beyond that, along a line at a constant radius, the plasma swirl angle decreases.

The continuous increase in the integrated axial flux in the downstream direction is not surprising since it is highly likely that arc currents are flowing throughout this region.⁽¹³⁾ The counterswirl in front of the cathode tip has been observed in the initial runs, but has not been definitely established since axial symmetry has not yet been checked there. However, there could be volume forces in the counterswirl direction in that region, due to an axial current and the radial magnetic field component. The symmetry of the flow at the exit plane has been measured and is very good. The probe was injected clear across a diameter: the probe body ex-

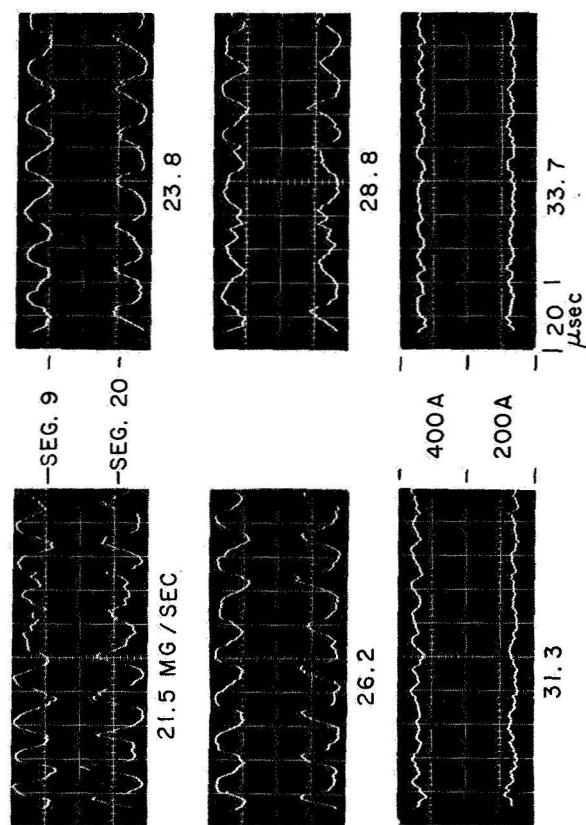


Figure 7. Segment current vs. time at various mass flow rates.
(arc current, 320 a;
tank pressure < 1μ; B_z = 1120 g)

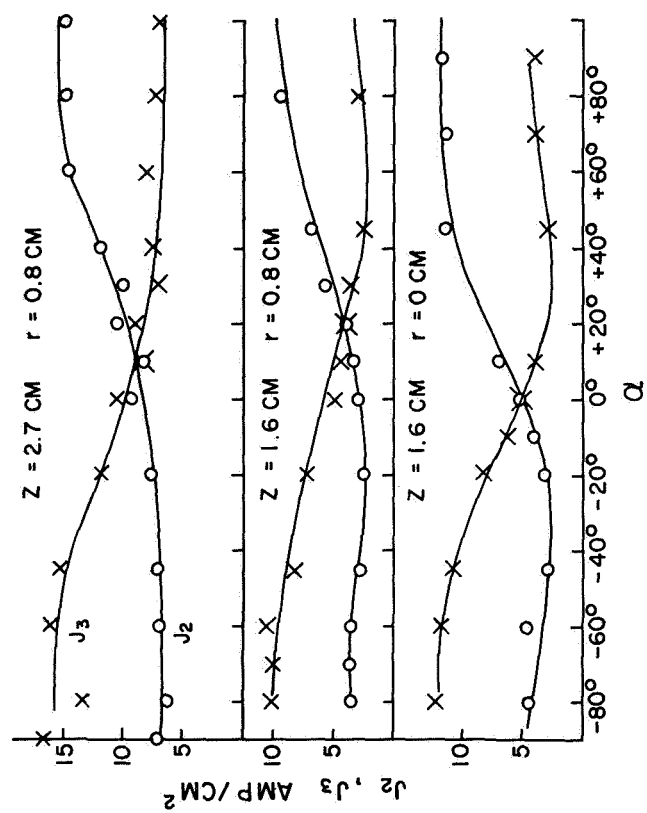


Figure 8. J_2 and J_3 vs. α .

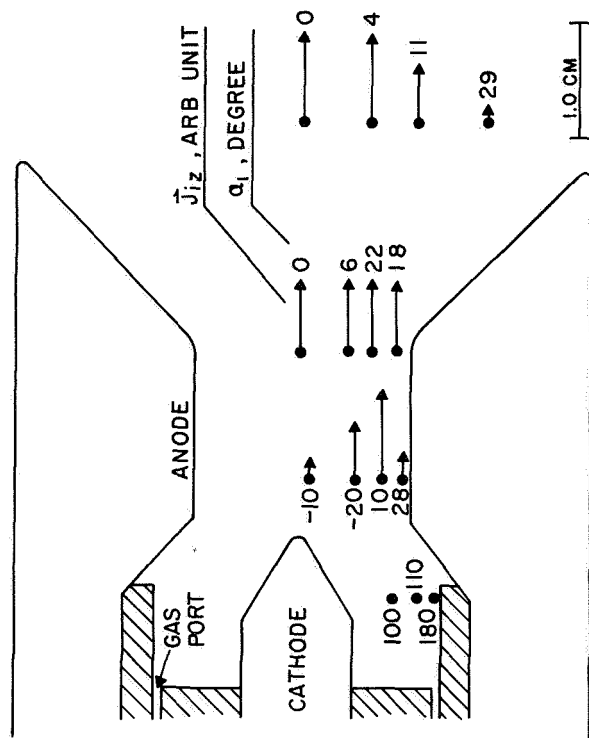


Figure 9. Ion flow in the θ - z plane vs. position: axial component and off axis angle.

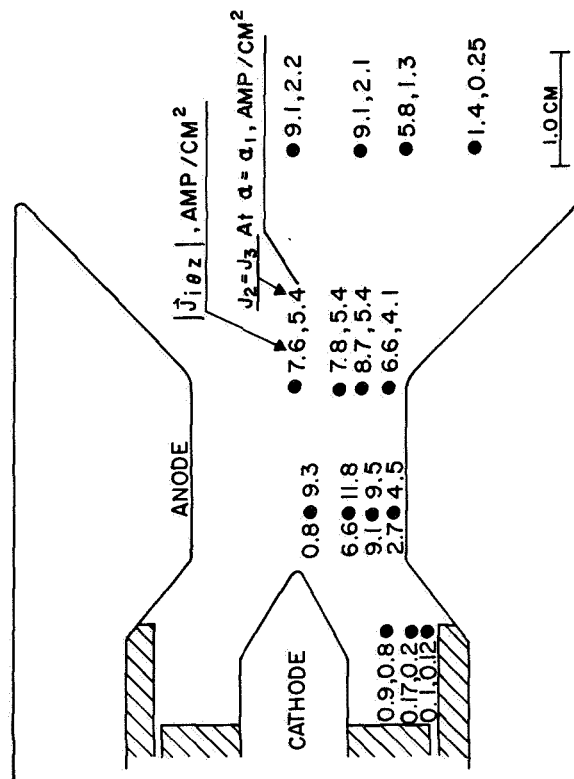


Figure 10. Ion flow in the θ - z plane vs. position:
magnitude of the directed and random flows.

tending across the jet to make measurements on the other side of the jet centerline did not disturb the symmetry.

The data of Figures 8-10 were taken with the thruster running in a no-spoke mode at 312 amp, 28 volt, 25 mg/sec of argon, and $B_z = 1120$ gauss. The thruster was very stable. The experiment was terminated earlier than planned when the thruster abruptly shifted into the mode pattern of Figure 5, where at those parameters, it is clearly in a spoke mode. This frustrating occurrence taught us about mode transition thresholds and initiated a search for a N to S transition region of a more permanent character. Following Schneiderman⁽¹⁴⁾ the cathode position was then changed.

2. Cathode at other Positions

The cathode was moved upstream to $z = 3.8$ cm. No grossly stable mode was found over the parameter range listed previously. Furthermore, the anode blackened, and some insulator chipped away. The insulator was cut back farther from the cathode tip for the next run, but the situation did not improve.

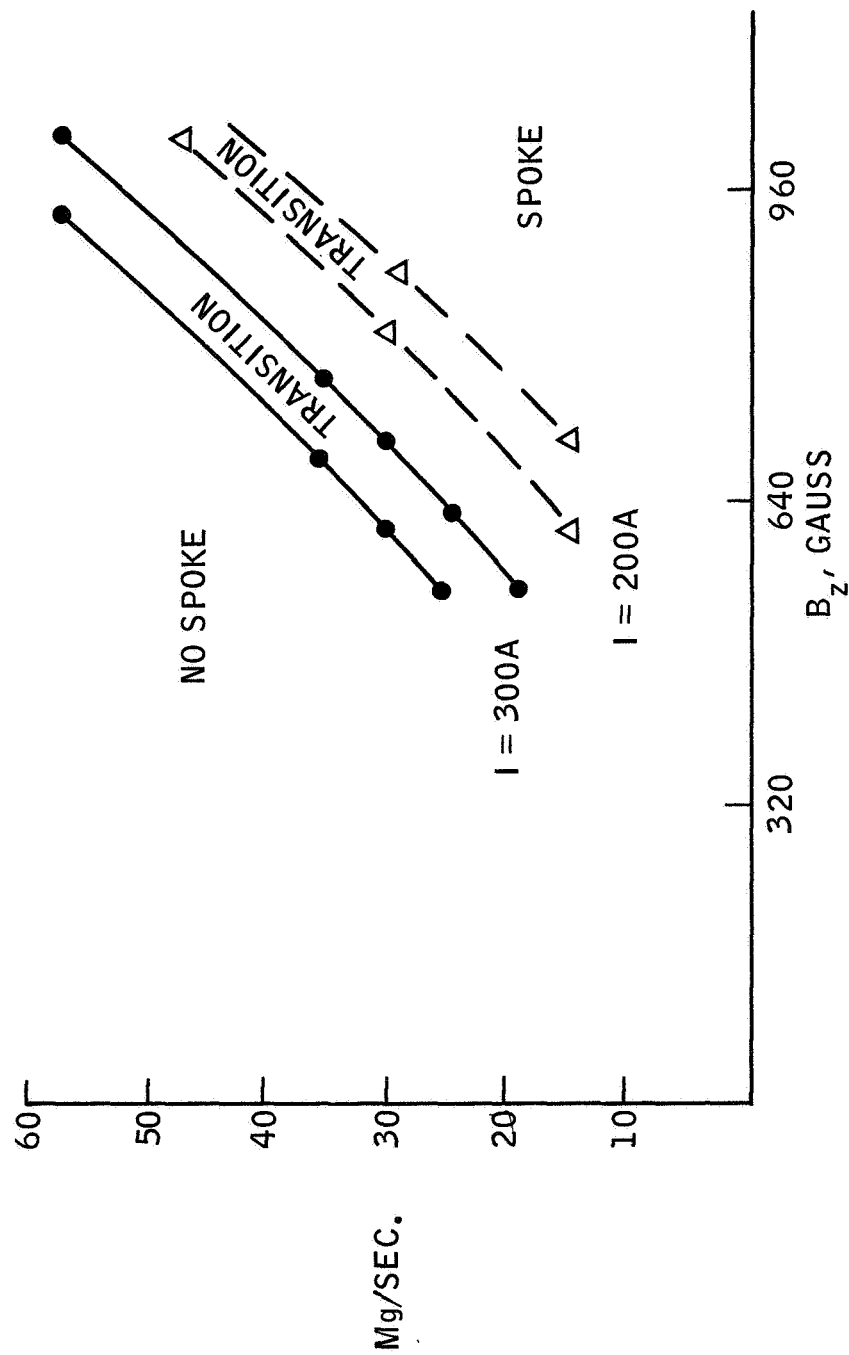
The cathode was then moved downstream to $z = 2.54$ cm. In this configuration, the engine has excellent stability. The spoke onset regions are very narrow, and have not drifted during 30 hours of running. The stability test period was carried out over several days and included many engine restarts under different conditions. The experimental measurements are repeatable to a few percent. This stability and repeatability is essential for detailed work on the differences of the spoke and no-spoke modes.

The parameters for spoke onset are given in Figure 11. In contrast to the data in Figures 5 and 6 with the cathode upstream, the magnetic field values for spoke onset are somewhat smaller. Also, now there are no gross engine fluctuations, even in the transition region. The mode transition occurs smoothly. The voltage and anode loss change continuously in the manner shown previously for the crossed data of Figure 6 and have nearly the same values.

3. Effects of Anode Segments and Geometry

Until recently, we have used either a solid anode or an anode with four segments. No significant effect of the segmentation has been observed. With the anode of three segments, shown in Figure 2, it is possible to have a very sensitive test of this conclusion. By use of the Rogowski coil signals, one can observe the time history of the current spoke transfer across the gap between segments 16 and 20. If no segment effect exists, then the sum of the Rogowski signals from 16 and 20 should be identical to the signal from segment 9, which has no such gap. Results again show no effect of the segmentation.

Figure 11. Spoke onset, argon: cathode at $z = 2.54$ cm.



Since the Rogowski coil detection efficiency is frequency dependent, and is zero for d.c. currents, it is important to also use d.c. shunts in these experiments. It has been found that the spoke frequencies are all near 100 kHz, the value for which the Rogowski coils were designed. The d.c. values of the current to the anode segments show an axisymmetric flow to the segments in either the spoke or no-spoke modes.

The general features of the experimental results in this report have also been found by Dr. Shih⁽¹³⁾ who operates a thruster with segments cut transversely to the thruster axis.

At the end of this contract, an anode was used briefly which was a right cylinder with its base exposed to the discharge, i.e., effectively a nozzle of 90° half-angle. Again, spoke onsets were found in the same parameter regions of Figures 5, 6 and 11. Thus it seems that anode geometry is not a sensitive factor.

IV. CONCLUSIONS

A continuous d.c. MPD engine has been run, very stably, with or without the presence of a rotating electric current spoke. In the no-spoke mode, the azimuthal swirl and axial flow of ions within the thruster have been determined by measuring the ion saturation current to a double planar Langmuir probe. The flow has no time dependence and at the nozzle exit plane is axisymmetric. Downstream from the cathode, the axial flow increases and the swirl decreases. The charge flow across the nozzle exit plane corresponds to 59% ionization of the propellant atom flow, if single ionization is assumed.

If the thruster has a rotating current spoke, then the ion flow is modulated at the spoke frequency. Initial results suggest that a strong plasma spoke then exists, closely coupled spatially to the current spoke. Detailed measurements have been made on such a plasma spoke in a pulsed arc.⁽⁸⁾

Quantitative interpretation of the magnitude of the ion saturation current to the Langmuir probe in such MPD arcs depends upon the ratio of particle mean free paths to the probe dimensions. The ratio is not expected to affect the identification of the swirl angle, because of the requirement that the probe electrodes, facing opposite directions, must measure identical currents when the faces are parallel to the flow. The relationship of the mfp to probe size has not been determined here. Yet, perhaps collisional effects are minor, since the probe response versus angular orientation in Figure 8 seems reasonable. In addition, the mfp appears to be large enough in a similar device⁽⁸⁾ to avoid interpretive problems with the data.

Because of the modulation of the ion flow, in the spoke mode, the negatively biased probe serves as a good spoke detector. This is especially true if the probe is within the thruster. Combined with the anode segment current measurements, the degree of azimuthal uniformity is then better established. The results here, then, confirm those of Malliaris⁽⁶⁾ and serve to remove some reservations about diagnostic techniques which he discussed. If a spoke exists, then the plasma flow is modulated at all places in the engine and the exhaust.

Parameter thresholds exist for triggering thruster mode changes from spoke to no spoke. The external magnetic field seems to be the most reliable trigger and small changes of 10 to 20% in its strength are sufficient. Transitions can occur smoothly or with engine fluctuations. In the latter case, an abrupt voltage mode change also occurs. Thermal efficiencies are slightly better on the spoke side of the transition region.

Each important result or feature found in a thruster with a segmented anode has always been checked and found in an identical thruster with a solid anode. No significant effect of the segmentation has been found.

Work in progress is planned to map the plasma flow in both the spoke and no-spoke modes. Of particular interest is the correlation of the thruster mode with the voltage drop across the anode sheath. It would seem most interesting to do this on both sides of a mode transition region that is narrow. This goal was initially hampered by a tendency for the transition parameter region to wander somewhat. However, by adjusting the cathode position, it has been found that the thruster runs very stably and its operating features are highly repeatable.

The existence of a narrow, repeatable transition region is ideal for the assessment of the significant differences between the spoke and no-spoke modes. So far we have observed that the following parameters do not change much during a mode change, at constant arc current, brought about by a change in the magnetic field: the arc voltage, the power loss to the anode, or the average azimuthal plasma flow.

V. ACKNOWLEDGEMENTS

The author appreciates the work of J. Koency and O. J. Neller in the design and construction of the apparatus and in assisting with the experiments. Also valuable were discussions held with Dr. P. Shih and Dr. R. Lovberg.

VI. REFERENCES

1. Nerheim, N. M. and Kelly, A. J., "A Critical Review of the MPD Thruster for Space Applications," Tech. Report 32-1196, Jet Propulsion Lab., Pasadena, Ca., Feb. 1968; also AIAA Paper No. 67-688.
2. Larson, A. V., "Experiments on Current Rotations in an MPD Engine," AIAA Journal, Vol. 6, No. 6, pp. 1001-1006, June 1968.
3. Connolly, D. J., Sovie, R. J., Michels, C. J., Burkhart, J. A., "Low Environmental Pressure MPD Arc Tests," AIAA Journal, Vol. 6, No. 7, pp. 1271-1276, July 1968.
4. Brockman, P., Burlock, J., and Hess, R. V., "The Effect of Various Propellants and Propellant Mixtures on a MPD Arc Jet," AIAA Paper No. 67-684, Sept. 1967.
5. Ekdahl, C., Kribel, R., and Lovberg, R., "Internal Measurements of Plasma Rotation in an MPD Arc," AIAA Paper No. 67-655, Sept. 1967.
6. Malliaris, A. C., "Oscillations in an MPD Accelerator," AIAA Journal, Vol. 6, No. 8, pp. 1575-1577, August 1968.
7. Fay, J. A., and Cochran, R. A., "An Actuator-Disc Model for Azimuthally Non-Uniform MPD Arcs," AIAA Paper No. 68-714, June 1968.
8. Lovberg, R., "Physical Processes in the Magnetoplasdynamic Arc," Fourth Semiannual Report, NASA Grant NGR-05-009-030, Univ. of Calif., San Diego, May 1968.
9. Leonard, S. L., "Basic Macroscopic Measurements," Plasma Diagnostic Techniques, ed. by Huddlestons, R. H., and Leonard, S. L., Academic Press, New York, pp. 8-14 (1965).
10. Chen, F. F., "Electric Probes," *ibid.*, pp. 113-200.
11. Brooks, D. R., "Use of Rotating Langmuir Probes in Flowing Plasmas," Rev. Sci. Instr., Vol. 37, pp. 1731-1732, Dec. 1966.
12. Burlock, J., Brockman, P., Hess, R. V., and Brooks, D. R., "Measurement of Velocities and Acceleration Mechanism for Coaxial Hall Accelerators," AIAA Journal, Vol. 5, No. 3, pp. 558-561, March 1967.
13. Shih, K., "Anode Current and Heat Flux Distributions in an MPD Engine," Paper 69-244, AIAA 7th Electric Propulsion Conference, Williamsburg, Va., March 1969.
14. Schneiderman, A. M. and Patrick, R. M., "Optimization of the Thermal Efficiency of the Magnetic Annular Arc," AIAA Journal, Vol. 4, No. 10, pp. 1836-1838, Oct. 1966.

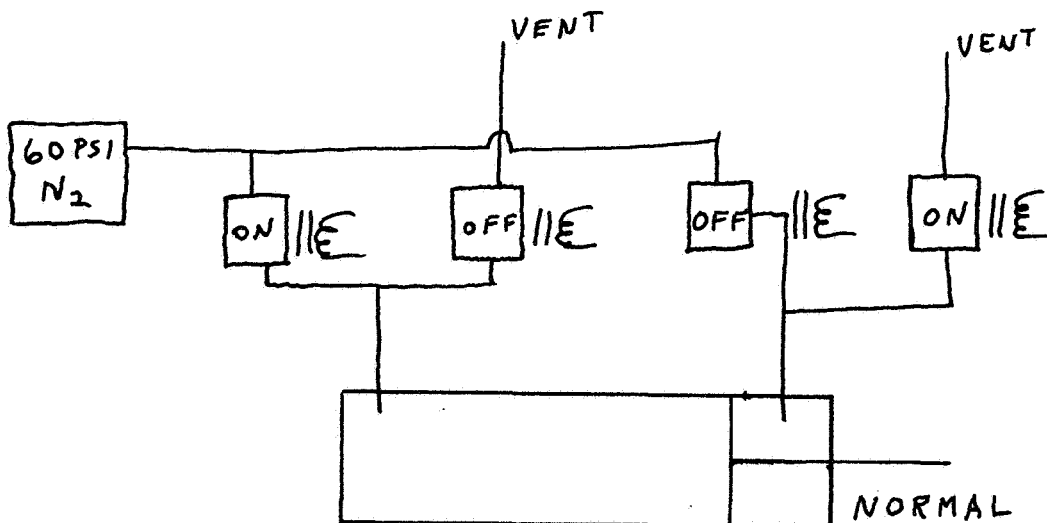
APPENDIX I

A description is given here of the mechanical apparatus for the quick insertion of a Langmuir probe into the thruster. The main features of the apparatus are shown in Figure 12. The rear view is shown in Figure 13 where the apparatus is on the tank mount located below the thruster. The probe is within the thruster. A close-up of the thruster region is shown in Figure 2.

The probe electrodes are held by an alumina oxide stem which is attached to a stainless steel shaft. The probe is normally withdrawn from the thruster and is at rest in a water-cooled housing. In operation, the shaft is driven by a lever arm which is moved by a pneumatic actuator. The shaft is guided in a straight line by teflon bearings. The shaft has several attachments for the purpose of position control, position readout, and scope triggering. The various parts are described next.

1. Pneumatic Actuator

A Hannifir series "S" cylinder was modified to give the desired stroke. It is controlled by four solenoid valves as seen below. The working gas is nitrogen at 60 psi. Figure 12 shows the cylinder in the normal position.



2. Lever

The turn-around-time of the actuator is too long. Therefore, the contact between the actuator and the lever arm is designed to act as a sear mechanism. The actuator and lever disengage before the probe reaches maximum insertion. Inertia carries the probe the last few millimeters of the stroke. The right end of the lever consists of two parallel rails which hold the probe. This construction allows the probe to be rotated about its own axis.

3. Stop Wheel

The probe travel is stopped and reversed by the stop wheel. The probe shaft passes through an annular slot near the circumference. Around the circumference, the slot depth changes in steps, thus providing seven probe stops, two millimeters apart, along the probe axis. The probe shaft is enlarged at one place to engage the wheel. The stop wheel determines the radial position of the probe within the thruster. It is visually set and read from outside the chamber. The probe is returned to its normal position by springs.

4. Probe Angle Control

The angular position of the probe is controlled by spline gears rotated by a motor-driven worm gear. A short spline gear attached to the probe shaft keeps the probe on any angle setting by sliding along the long spline gear.

5. Probe Angle Indicator

This shows the angle of the probe electrodes with respect to the thruster axis, and is read visually from the outside of the vacuum chamber.

6. Apparatus Mount

The mount is adjustable in three mutually perpendicular directions, one of which is parallel to the thruster axis. The base of the mount is an electrical insulator.

7. Material

Nonmagnetic materials were used throughout. Platinum was used for the Langmuir probe electrodes.

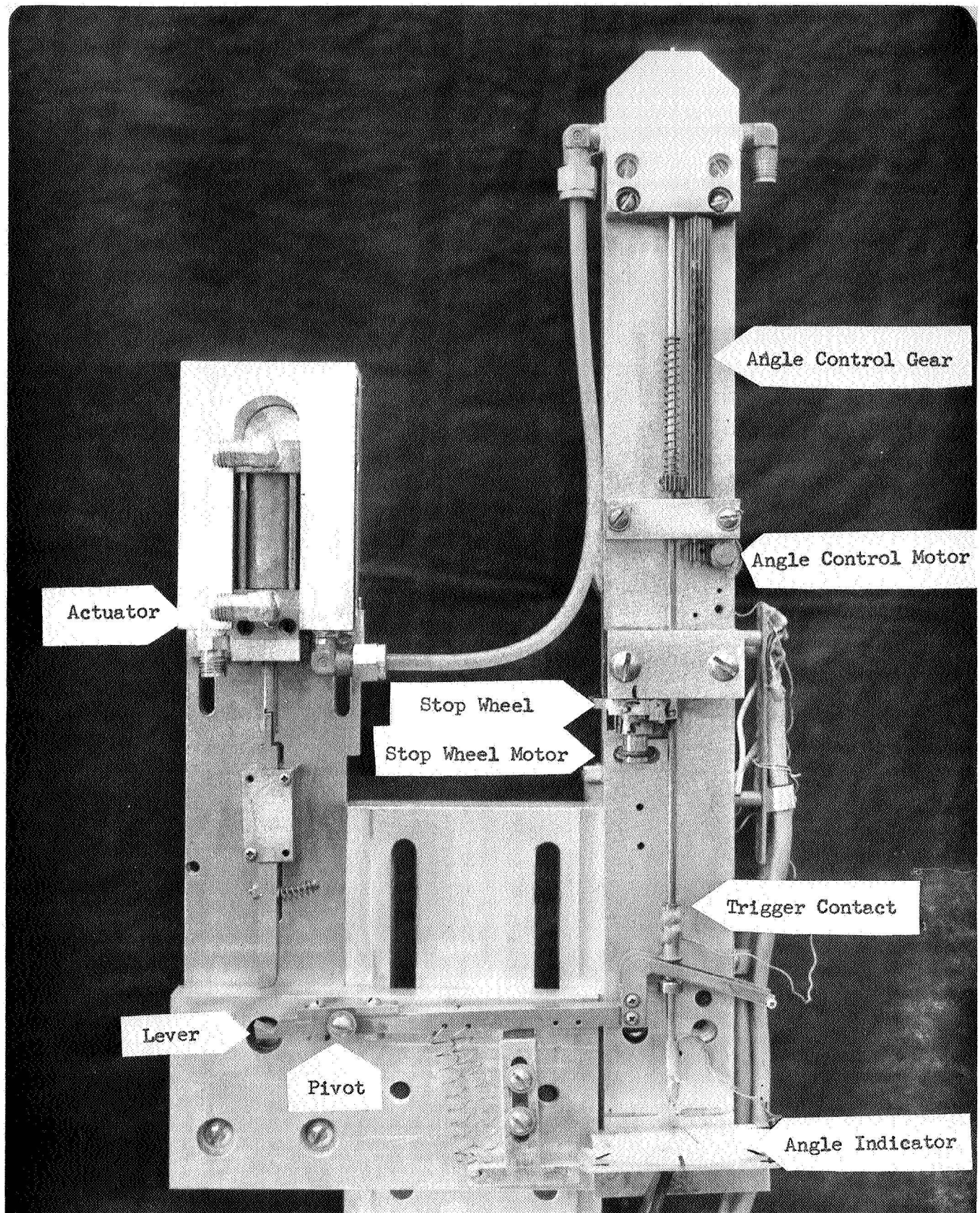


Figure 12. Probe insertion apparatus.

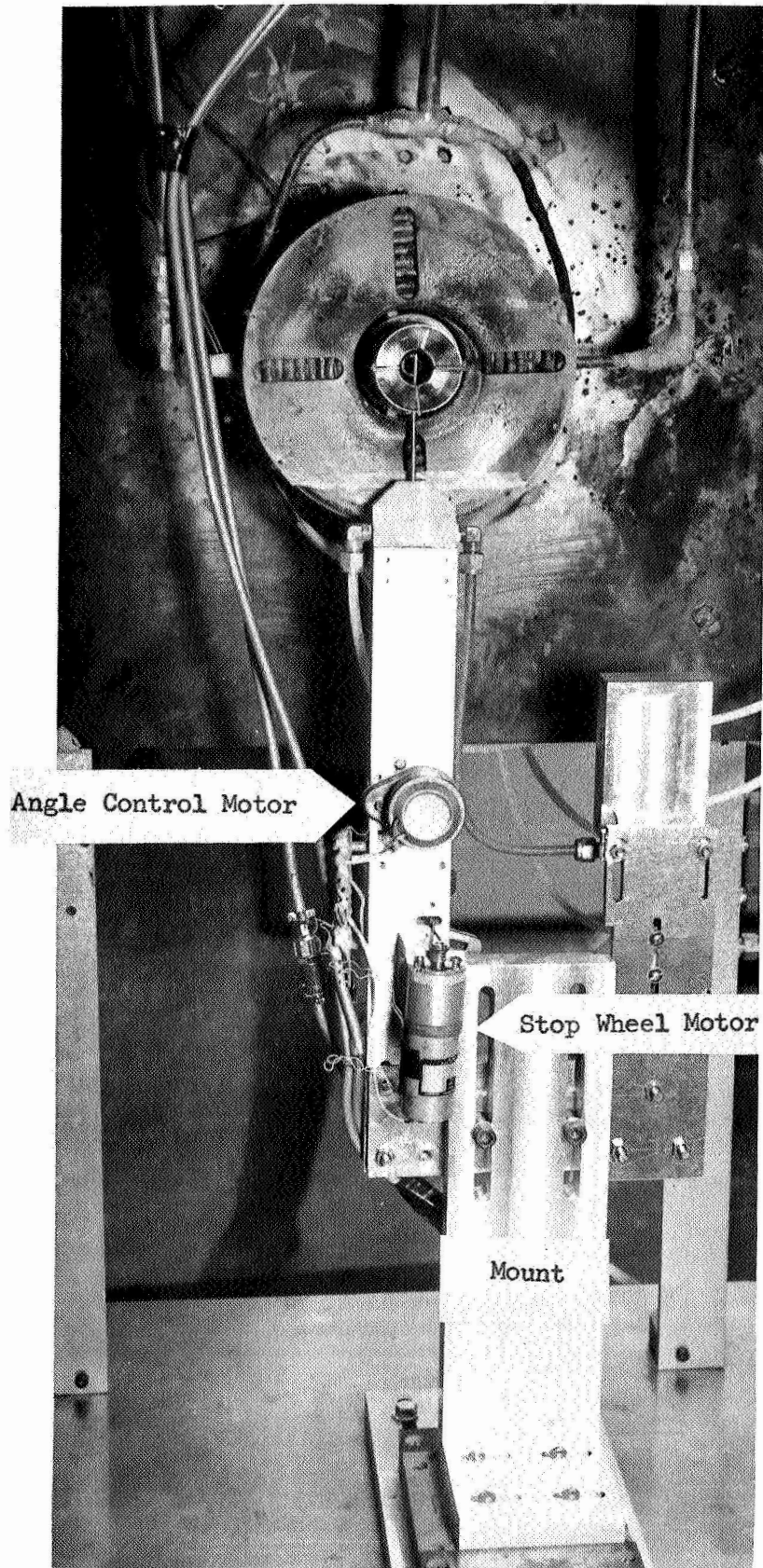


Figure 13. Experimental set up.